Title: Parametric modulation of the blink reflex provides an individual difference measure of trigeminal sensitivity

Running head: Trigeminal blink sensitivity function

Author(s):
Eric Kaiser[1†]; Edda B Haggery[1†], Dena P Garner[2], Vatinee Y Bunya[3], Geoffrey K Aguirre[1*]

[†]These authors contributed equally

[*]**Corresponding Author:**
Geoffrey K Aguirre
3400 Spruce Street, Philadelphia, PA 19104
aguirreg@upenn.edu

Affiliation Information for Authors:
[1]Department of Neurology, Perelman School of Medicine, University of Pennsylvania, Philadelphia, PA 19104
[2]Department of Health and Human Performance, The Citadel, Charleston, SC 29409
[3]Scheie Eye Institute, Perelman School of Medicine, University of Pennsylvania, Philadelphia, PA 19104

Key Points

- Stimulation of the cornea and skin around the eye evokes an involuntary eyelid closure, termed the trigeminal blink reflex
- There has been limited study of how variation in the intensity of stimulation modulates the properties of the blink reflex
- We have developed a psychometric measure of the trigeminal sensitivity function evoked by log-spaced intensities of an airpuff stimulus directed at the eye
- The parameters of this function reveal a systematic difference in threshold sensitivity between the eyelids contralateral and ipsilateral to the side of stimulation and substantial and reliable individual differences in overall sensitivity
- A psychometric measure of trigeminal sensitivity can inform models of the neural circuits that generate the response and be used in future tests of altered trigeminal function in clinical populations

Abstract

The trigeminal blink response is a familiar and easily evoked brainstem reflex. Despite a long history of clinical and research investigation, there has been limited study of how parametric manipulation of the intensity of somatosensory stimulation modulates the evoked response. The goal of this study was to measure the psychometric trigeminal sensitivity function and to test the resulting model parameters for differences between the eyelids contralateral and ipsilateral to the side of stimulation, and to test for individual differences in sensitivity. We measured the ipsilateral and contralateral blink in 17 healthy, adult participants in response to airpuffs delivered to the cornea over a range of five, log-spaced intensities (3.5 - 60 PSI). The temporal lid position vector was decomposed into amplitude, velocity, and shape components. We found that variation in blink amplitude was well fit with a two-parameter Weibull cumulative density function of log stimulus intensity. There was a reliable decrease in threshold sensitivity of the contralateral as compared to ipsilateral eyelid. This decrease was consistent across participants despite substantial individual differences in the threshold and slope of the overall sensitivity function, suggesting that the laterality effect arises subsequent to individual differences in the neural circuit. We conclude that a parametric measure of trigeminal sensitivity is a promising tool for examining neural mechanisms that modulate this response, including in various disease states.

Introduction

The trigeminal blink reflex is an easily evoked, clinically relevant measure of brainstem function. The cornea of the eye and periorbital skin are innervated by the ophthalmic (V1) division of the trigeminal nerve. In the brainstem, the principal sensory nucleus of V receives light-touch sensation from V1, while the nucleus caudalis receives both light touch and nociceptive afferents (May & Porter, 1998). Both of these nuclei project to local brainstem circuits that serve reflexive functions, including eye blink (May & Warren, 2021).

There is a long history of quantitative measurement of the human trigeminal blink reflex, with the most used approach being unilateral electrical stimulation of the supraorbital nerve or cornea, and electromyographic (EMG) measurement of the binocular orbicularis oculi response. Generally, the amplitude or latency of the response is measured for a fixed stimulus intensity, or the threshold stimulus if found that evokes a criterion EMG response. There has, however, been relatively little study of the effect of variation in somatosensory stimulus intensity upon the evoked response. It is usually the case that there exists a range of log-spaced changes in stimulus intensity that evoke linear changes in perception or physiologic response, following the Weber-Fechner law. A focus upon measurement at response threshold can obscure individual and population differences. For example, two groups may initiate a physiologic response at the same threshold but differ in the amplification of that response with further increases in stimulus intensity. Further, examination of the full sensitivity function, and how this function interacts with other experimental variables, may be revealing as to the organization of the underlying neural system.

Motivated by these observations, we develop here a quantitative measure of the blink response evoked by parametric variation of a somatosensory stimulus. We used high-speed infrared cameras to record lid position following puffs of air directed towards the cornea at log-spaced pressure intensities. We measured how variation in stimulus intensity modulated features of the blink response. We then tested the ability of these data to reveal reliable

differences in the sensitivity functions of the ipsilateral and contralateral blink response, individual differences in the sensitivity of the trigeminal system, and changes in blink responses across trials as a measure of habituation.

Methods

Participants

In a pre-registered experiment (https://github.com/gkaguirrelab/preregistrations/tree/master/blink_2021), we studied 17 participants recruited and tested by BlinkTBI Inc. These participants were recruited from The Citadel in Charleston, SC and from non-clinical settings in the surrounding Charleston community. Participants were at least 18 years of age, had no history of concussion within the past 5 years, and denied a history of recurrent headache. This study was approved by The Citadel Institutional Review Board and all participants provided written consent.

The analyses presented here deviates from that proposed in our pre-registered protocol. The supplementary materials present results that follow as closely as possible the pre-registered approach.

Operation of the device

Blink responses were measured using a custom-modified blink reflexometer (The EyeStat device, Gen3, Blink TBI Inc) positioned over the eyes of the seated subject. During each of many ~30 second acquisitions, the device directed 8 airpuffs from a pressurized CO_2 cartridge to the cornea and lateral canthus with the left or right eye selected randomly on each of the 8 trials. The inter-stimulus-interval was jittered to reduce the ability of the participant to anticipate the timing of the stimulus with at least 3 seconds between stimuli. The eyes were illuminated with a ring of IR-LEDs that produced a corresponding ring of glint reflections on the tear film. A pair of high-speed IR cameras (300 Hz, 800 x 600 pixels) were used to measure the timing of obscuration of the glints by the movement of the eyelids. Recordings were made of the

movement of the eyelid ipsilateral and contralateral to the side on which the stimulus was delivered. Microphones adjacent to the lateral canthus detected the airpuff, and the time of the arrival of this pressure wave was used to sync recorded responses across trials.

During testing, subjects steadied themselves to receive the stimulus by holding the legs of a tripod that supported the device. Room lights were left on during the session, although the field of view of the subject was dark during data acquisition while their face was placed within the device.

The device used in this study was custom modified by the manufacturer to externalize pressure regulation. The CO_2 cartridge was connected by rigid tubing to an external pressure regulator (Reg3000x, Leland Gas Technologies, South Plainfield, NJ), and then returned by tubing to the EyeStat. Accuracy of specified air pressure levels was monitored with a National Institute of Standards and Technology calibrated device (PressureMon2000, RegCo, Miami Florida), which is certified to be accurate within ±0.2 pounds per square inch (PSI).

Data collection

The stimulus intensity was varied in separate acquisitions between five different, log-spaced pressure values. A set of 26 acquisitions were obtained in each of two sessions, with the order of pressure values following a pseudo-random, counterbalanced sequence de Bruijn sequence (Aguirre *et al.*, 2011): [3, 3, 0, 2, 4, 4, 2, 0, 1, 3, 1, 1, 0, 4, 3, 2, 2, 3, 4, 1, 2, 1, 4, 0, 0, 3]; where 0 = 3.5 PSI, 1 = 7.5 PSI, 2 = 15 PSI, 3 = 30 PSI, and 4 = 60 PSI. To reduce the influence of non-selective startle responses, data from the entire first acquisition were discarded, as was the first trial of each acquisition. A total of 10 acquisitions were therefore obtained at each of the five pressure levels, with each acquisition containing seven retained trials. The operator of the device attempted to achieve the desired PSI value within ±1 PSI, and the actual, achieved stimulus intensity was recorded for each acquisition. The unsigned mean

deviation from nominal values was 0.31 PSI, and in all cases did not exceed 1 PSI. For one participant three of the acquisitions included 4 trials instead of 8 due to operator error.

There was a 30 - 60 second break following each acquisition. Each session was approximately 50 minutes in duration, and the two sessions were separated by 1 to 5 days.

Data pre-processing

The raw data consisted of infrared videos of the eyelids during each trial. Initial processing of these videos was conducted by Blink TBI Inc. using proprietary software. This first stage of analysis provided a measure of lid position during each trial with 3.5 msec temporal resolution, with all trials aligned to the time of arrival of the stimulus at the eye. All subsequent analyses were performed using custom MATLAB software (Mathworks, Natick, Massachusetts). The data and code needed to reproduce the analysis and figures presented here are publicly available (https://github.com/gkaguirrelab/blinkCNSAnalysis).

The lid position over time was obtained for each subject for each stimulus intensity level, averaging over all remaining trials and acquisitions. The raw measurement of lid position in units of pixels was converted to a proportion of full eye closure by scaling all responses by the maximum excursion observed for that subject and session. Full lid closure was observed for all subjects at either the 30 or 60 PSI stimulus. This normalization accounted for variation in the absolute size of the palpebral fissure across subjects and in the precise distance of the eye from the infrared cameras.

The primary analyses of the study examined the set of 170 average lid position vectors obtained from the 17 subjects at each of the 5 pressure levels, measured from the eye ipsilateral and contralateral to the stimulus, averaged across trials and acquisitions.

Three-component model of temporal response

A model of the blink response over time was created to allow the temporal vector of lid position to be summarized with a set of coefficients. The first component of the model was the

average profile of lid position over time, combined across subjects, pressure levels, and the ipsilateral and contralateral eye. The second component was the first derivative of average lid position. Next, a set of residual vectors was obtained by regressing each of the 170 vectors of lid position upon these first two components. The set of residuals was then subjected to a principal components analysis, and the first eigenvector was retained as the third component of the model of temporal response. These three orthogonal components account for, respectively, variation in the amplitude, velocity, and shape of the blink response.

A simple linear regression was then used to fit this three-component model to each lid-position vector, yielding three coefficients. The effect of stimulus intensity upon the coefficients was then examined, as well as the effect of other variables.

Psychometric function relating blink amplitude and stimulus pressure

A Weibull cumulative distribution function (Wichmann & Hill, 2001) was used to model the effect of log-transformed stimulus pressure upon the coefficients that measured the amplitude of blink response (expressed as the proportion of a full blink). Two parameters controlled the shape of the fit, corresponding to the maximum slope of the function and the pressure at which 50% eye closure was predicted. This function was fit to the amplitude coefficients obtained from each subject using the MATLAB *fmincon* function. A comparison of the fit parameters between the ipsilateral and contralateral eye was performed with a paired t-test across subjects.

A bootstrap resampling procedure was used to estimate the standard error of the mean of the parameters within subject. In this procedure, the set of 10 acquisitions obtained at each pressure level for a subject were randomly sampled with replacement, then the coefficients of the three-component model obtained for the synthesized average blink response, and then the parameters of the Weibull fit derived. The standard deviation of parameter values observed over 1,000 resampling iterations was taken as the standard error of the parameter mean.

Examination of habituation effects

For each subject, the blink response vectors for sequential trials within each acquisition were obtained and averaged over stimulus levels. After fitting with the three-component temporal model, the coefficients were examined for an effect of trial number.

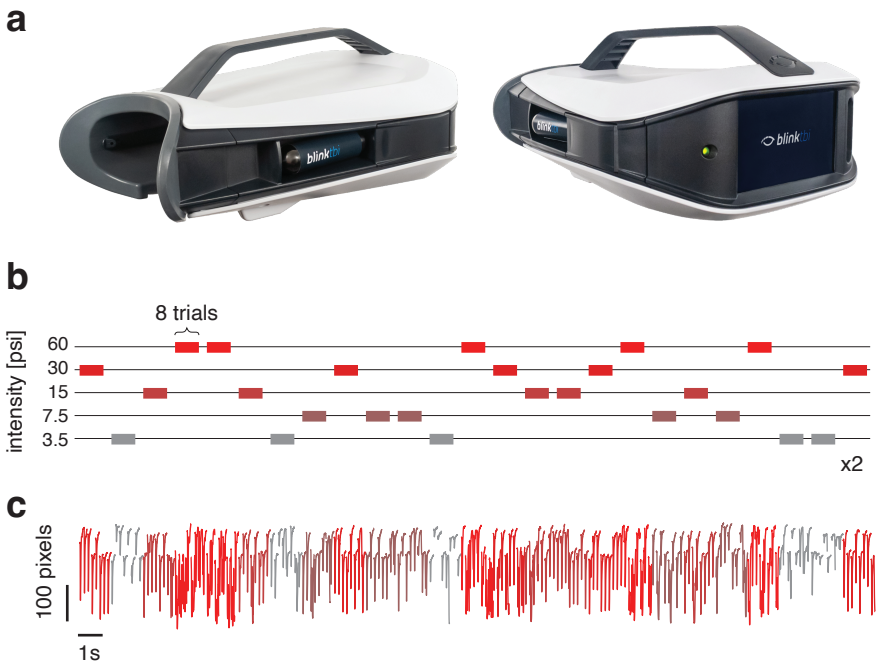

Figure 1. Experiment overview
(a) Blink responses were measured using an Eyestat Gen3 device, with custom modifications (not shown) to externalize pressure regulation. The participant placed their eyes within the mask assembly. **(b)** Counterbalanced pressure sequence. Each dash represents a single acquisition that presented a sequence of 8 airpuff trials. The air pressure used for the 8 trials was varied across acquisitions as shown. The entire sequence was administered twice. **(c)** Lid position over time obtained for Subject 14594. The data from each acquisition is color coded to indicate stimulus intensity, following the convention shown in panel b.

Results

Participants and data properties

We collected measurements from 17 participants who were recruited from a non-clinical setting and who denied a history of recurrent headache and acute or persistent symptoms from traumatic brain injury. Nine of the subjects were women, and the mean age of all participants was 25 (range 20 to 32).

Each subject was studied using a custom-modified blink reflexometer (Figure 1a) that directed puffs of air at the cornea and lateral canthus. A total of 10 acquisitions of 8 airpuff trials was obtained at each of five, log-spaced pressure intensities with the order of acquisitions following a counter-balanced sequence (Figure 1b). IR video recordings of the eye ipsilateral and contralateral to the stimulus provided a measure of lid position over time (Figure 1c). From these recordings, the average blink response was obtained for each participant for each of the five stimulus intensities.

Our overall approach to the analysis of these data was to create a low-dimensional representation of the temporal components that constitute the blink response and then examine how the size of these components changed with stimulus intensity.

Blink responses are well described by three temporal components

We combined the responses from the eyelids ipsilateral and contralateral to the stimulus and examined the evoked blink response across participants and stimulus intensity levels. Figure 2a presents these data as a temporal raster plot with each evoked response in a row, and the grayscale level indicating the depth of lid movement. A similar general pattern was seen across subjects (grouped blocks) and stimulus intensity levels (increasing stimulus intensity across rows within a block). Following the stimulus arrival at the cornea (vertical blue line), a blink of 100-200 msecs duration was initiated after a latency of 30-50 msecs. With increasing stimulus intensity, latency appeared to decrease, and blink duration and depth appeared to

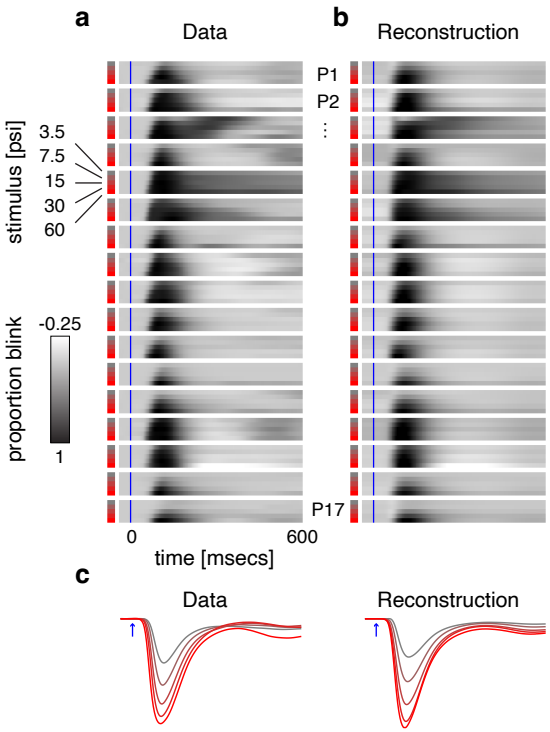

Figure 2. Observed and modeled blink responses **(a)** The raster plot presents the temporal profile of lid position (averaged across acquisitions and ipsilateral and contralateral eyes) on each row, with blink depth indicated by grayscale shading. The responses to each of the five stimulus intensity levels are grouped together with each block running vertically corresponding to a different participant. The time of stimulus arrival at the cornea is indicated by a blue line. **(b)** The reconstruction of the data produced by the three temporal component model. There is good agreement between the reconstruction and the original data. **(c)** *(Left)* The average (across participant) blink response evoked by the five different stimulus intensity levels, with color indicating airpuff level from gray (3.5 PSI) to red (60 PSI). The blue arrow indicates the time of arrival of the airpuff to the cornea. *(Right).* The fit to these data provided by the 3 component temporal model.

increase. Beyond these similarities, we also observed individual variation in the size and timing of the response and in the degree to which the response changed with stimulus intensity.

We created a low-dimensional temporal model of the blink response to describe this regularity and variation (Figure 3). The first component of the model (black) is simply the average lid position across all participants and stimulus levels and serves to capture the amplitude of the blink response. The second component (blue) is the first derivative of lid position and captures variation in the velocity and latency of the blink onset. The final “shape” component (gray) reflects variation in the overall shape of the evoked response, including individual differences in the tendency to hold the lid in a partially closed or more open state following the primary blink. Weighted combinations of these three components were used to fit a lid position vector, yielding three coefficients that summarized the response.

We fit the 85 average blink responses (17 participants x 5 stimulus levels) with the three-component temporal model. The reconstructed responses (Figure 2b) were a good match to the original data and accounted for 95% of the variance. The agreement between the data and the

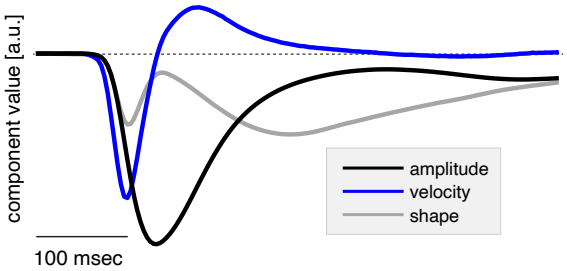

Figure 3. Temporal model components
Lid position vectors over time were fit using a three-component temporal model. These components corresponded to the amplitude of the blink (black), the first-derivative of amplitude and thus velocity (blue), and a third component that captured residual variation in shape (gray).

reconstruction can also be seen in the average (across subject) blink response at each stimulus pressure level (Figure 2c).

Blink amplitude and velocity increase with stimulus intensity

We examined the value of the fit coefficients averaged across participants and sides (ipsilateral and contralateral) for each stimulus intensity level. This revealed a systematic effect of airpuff pressure upon blink response (Figure 4). Blink amplitude (expressed as the proportion of a complete blink) increased with stimulus intensity, with a roughly linear increase in blink depth related to log changes in stimulus pressure. Above 30 PSI, however, this function appeared to plateau. Blink velocity also increased with stimulus intensity: log changes in stimulus intensity led to roughly linear increases in blink velocity, reducing the latency of the response by about 15 msecs over the entire stimulus range. By contrast, no systematic relationship between stimulus intensity and the shape component was seen.

These findings confirm that aspects of the trigeminal blink response undergo parametric modulation with stimulus intensity. In subsequent analyses, we focus upon properties of the amplitude of the blink response, motivated by the reliability of the effect of stimulus intensity upon this measure, and the interpretability of the measure in terms of proportion of full lid closure.

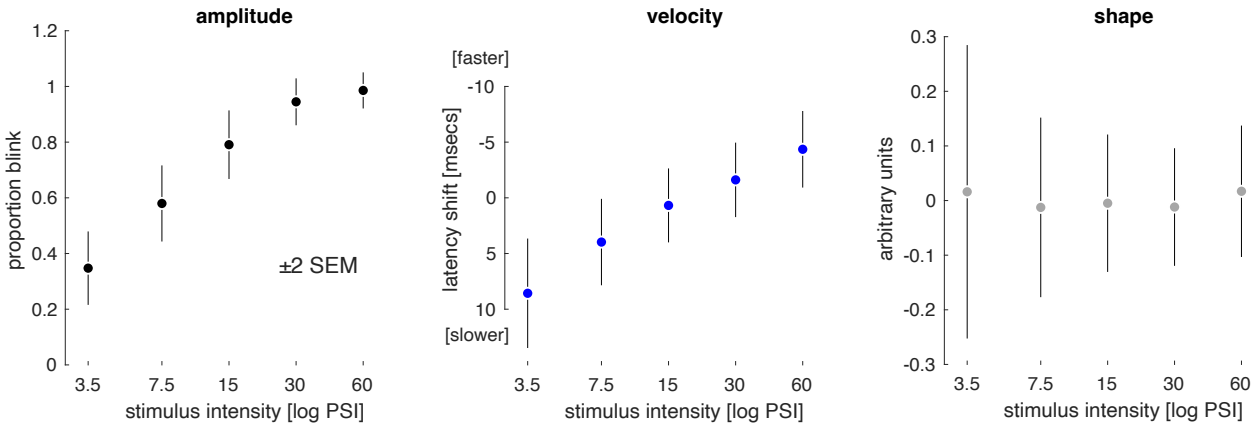

Figure 4. Coefficient values by stimulus intensity
Each plot presents the mean (across participants) coefficients for the three temporal components (amplitude, velocity, and shape) as a function of stimulus intensity (log PSI). Error bars are ±2 standard error of the mean across participants.

The contralateral blink response is subject to an increased stimulus threshold

The analyses up to this point combined the blink response measures from the eyelids ipsilateral and contralateral to the stimulus. We next tested if there are consistent differences in the sensitivity of the ipsilateral and contralateral response to trigeminal stimulation. We obtained the average amplitude coefficients across subjects for each stimulus level, separately for the ipsilateral and contralateral eye (Figure 5a). The measurements from each eye across pressure levels was then fit with a non-linear psychometric function (the Weibull cumulative distribution function). These fits provided a good account of the data and revealed that the intensity response function measured from the contralateral eye was shifted to the right as compared to the response from the ipsilateral eye. This property of the data indicates that generally higher intensity stimuli were required to evoke the same degree of lid closure in the contralateral eye as compared to the ipsilateral.

The Weibull function is under the control of two parameters that correspond to the stimulus intensity required to produce a 50% eye closure (the “half response threshold”), and the maximum slope of the change in eye closure with log changes in stimulus intensity. To assess the reliability of the difference in response between the ipsilateral and contralateral eye,

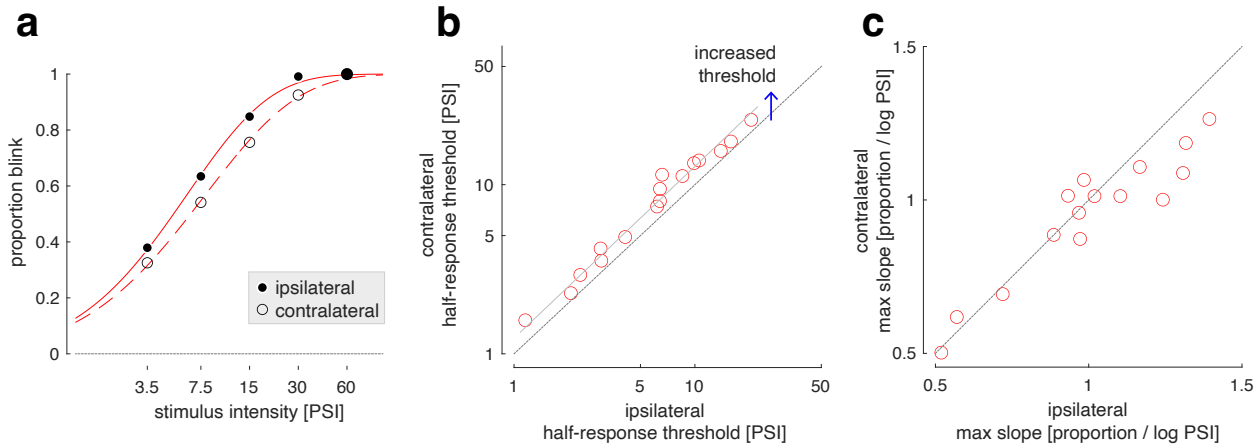

Figure 5. Ipsilateral versus contralateral blink responses.
(a) The mean (across participant) amplitude coefficients as a function of stimulus intensity, obtained separately for the eyelid ipsilateral (filled circles) and contralateral (open circles) to the stimulus. Amplitude is expressed as the proportion of a full eyelid closure. The points are fit with Weibull cumulative distribution function (red lines). **(b)** The psychometric function was fit to the amplitude data for each participant and side (ipsilateral and contralateral), yielding two parameters (half-response threshold and maximum slope). Here, each plot point indicates the half-response threshold parameters measured for a particular participant from the ipsilateral and contralateral eyelid. A linear fit to the set of points (gray line) is parallel to and shifted upwards from the unit slope (dashed line), corresponding to an ~0.1 log unit increased half-response threshold value measured from the contralateral as compared to the ipsilateral eyelid. **(c)** Each plot point indicates the maximum slope parameter value obtained from the ipsilateral and contralateral eyelid from each participant.

we fit the amplitude coefficient data for the ipsilateral and contralateral eyelid separately for each participant. Figure 5b presents the half-response threshold values obtained for each participant from the ipsilateral and contralateral eyelid. While a wide range of values was seen, the plot points for all 17 participants were displaced ~0.1 log units above the unit slope line. A paired t-test across subjects of this measure between the contralateral and ipsilateral eye showed a significant difference (t[16 df] = 8.29, p = 3.4e-7). This finding reveals that, across participants, there was a notably consistent, ~25% decrease in the threshold sensitivity of the response of the contralateral eyelid to trigeminal stimulation as compared to the ipsilateral eyelid.

Figure 5c presents the maximum slope of the psychometric function measured from the ipsilateral and contralateral eye for each subject. A wide range of values was again seen, although in this case the plot points did not systematically depart from the unit slope line,

indicating a similar measurement from the two eyes. A paired t-test indicated that there was not a highly reliable difference in the slope value between the eyes (t[16 df] = 2.17, p=0.045).

We examined if the timing and shape of the blink response of the ipsilateral and contralateral eye differed. Across subjects and averaged across pressure levels, the velocity coefficient value was larger in the response from the contralateral eye as compared to the ipsilateral eye (t[16 df] = 3.83, p = 1.5e-03), corresponding to an approximately 4 msec relative delay in the response of the contralateral eye. The blink response was also consistently narrower in time in the contralateral eye as compared to the ipsilateral eye, which was reflected in a difference in the shape coefficient (t[16 df] = 9.82, p = 3.5e-08).

Reliable individual differences in sensitivity parameters for blink amplitude

We next examined individual variation in the relationship between stimulus intensity and blink amplitude. Given that the difference between the ipsilateral and contralateral blink response was both small and consistent across individuals, we considered the blink responses averaged across the two eyelids. Figure 6a presents the fit of the non-linear Weibull function to the blink response amplitudes for each participant, ordered by the half-response threshold value obtained. For all participants, the psychometric function provided a good account of the effect of stimulus intensity upon blink amplitude. Across subjects, however, there was substantial variation in the form of the psychometric function. This variability can be seen both in the half-response threshold of the function (blue dotted lines), and in the maximum slope (steepness) of the fits.

The two parameters of the Weibull fit define for an individual the sensitivity of their blink response to varying trigeminal stimulation. Figure 6b plots the value of these two parameters for each participant, accompanied by the bivariate ellipse that indicates the standard error of the mean for the parameter estimates (obtained by bootstrap resampling across the 10 acquisitions at each stimulus level). Differences between individuals were substantially larger than the

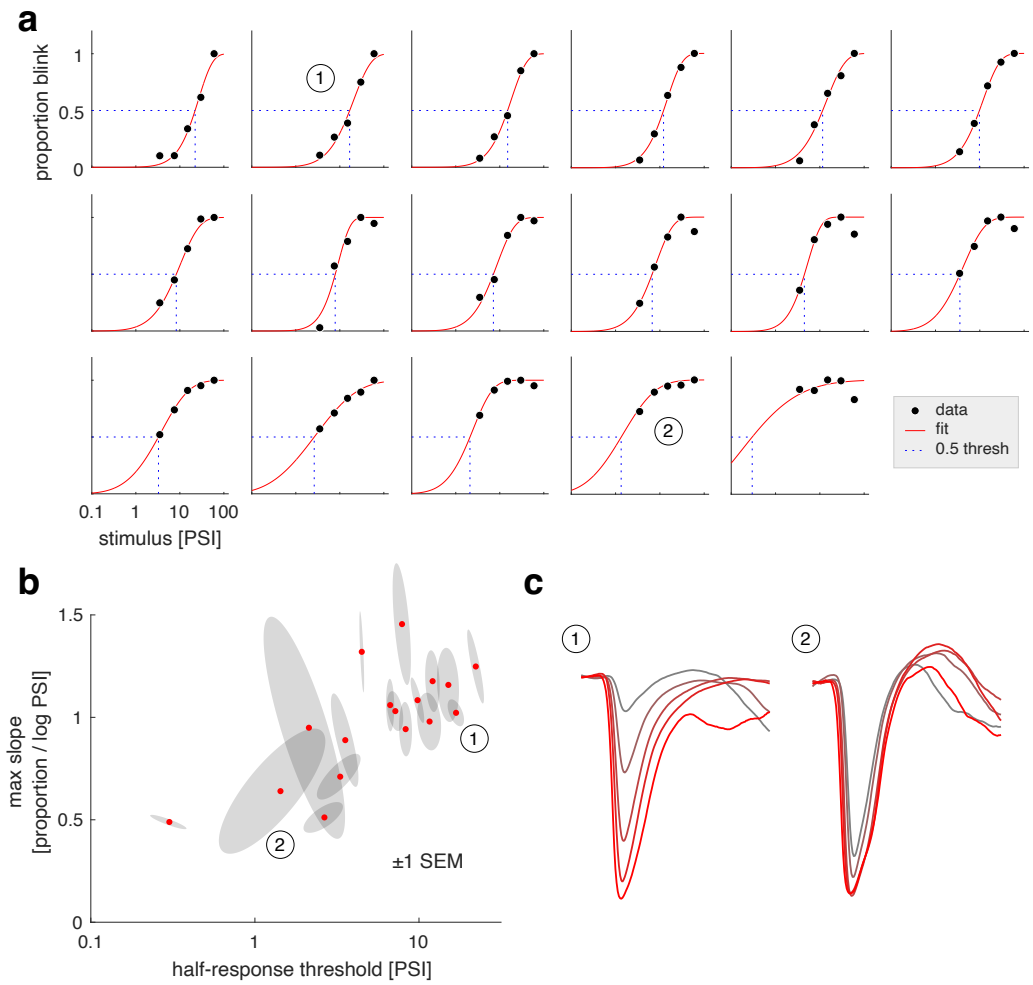

Figure 6. Individual differences in psychometric properties of blink amplitude.
(a) Each sub-plot presents the amplitude coefficients for a participant as a function of stimulus intensity, averaged over acquisitions and the contralateral and ipsilateral eye. The fit of a Weibull cumulative distribution function is shown (red line), as is the half-response threshold value (dashed blue lines). Two example participants are identified with circled numbers, and these same participants are so indicated in subsequent panels. **(b)** The relationship between the half-response threshold and maximum slope parameters for each participant (red dots), surrounded by the bivariate normal distribution at one standard error of the mean obtained by bootstrap resampling across the 10 acquisitions (gray ellipses). **(c)** The average lid position plots at each stimulus intensity for two example participants (line color follows the convention of Figure 1).

measurement uncertainty. There was a positive correlation between half-response threshold and maximum slope across participants (r = 0.73). The underlying differences in the blink response across stimulus levels is shown for two example participants in Figure 6c.

For roughly half of the participants, a decline in the amplitude of the blink was noted between the 30 and 60 PSI stimulus levels. Post-hoc examination of the data indicated that this

phenomenon resulted from some subjects narrowing their palpebral fissure (i.e., squinting) during the set of eight trials with the highest stimulus intensity. This partial closing of the eye resulted in a smaller excursion of the lid in response to the stimulus.

Changes in blink amplitude and velocity with repeated stimulation

Finally, we examined how the properties of the blink response changed over the 8 stimuli that were presented in rapid succession within each acquisition. For each participant, we fit the 3-component temporal response model to the average response across stimulus intensity, acquisitions, and sides, separately for each of the 8 trials. Figure 7 shows that across trial number, there was a decrease in the amplitude of the blink response, a slight increase in velocity, and no change in blink shape. These changes followed an exponential form, with the largest change in response coefficients being present between the first and second trial. For this reason, the analyses we pursued here discarded the response from the first trial in each acquisition.

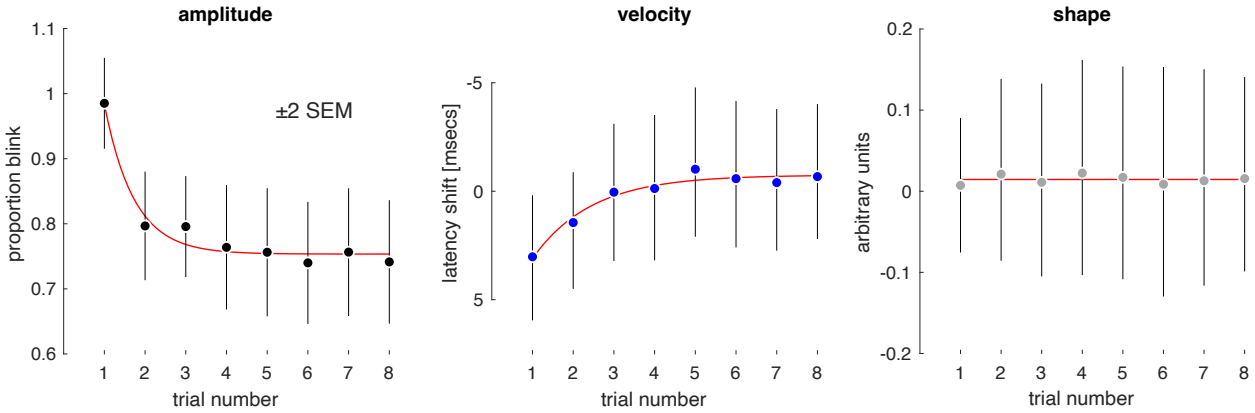

Figure 7. Coefficient values by trial number
Each plot presents the mean (across participant) coefficients for the three temporal components (amplitude, velocity, and shape) as a function of trial number. Error bars are ±2 standard error of the mean across participants. The fit of an exponential function is shown (red line).

Discussion

We have developed a measure of parametric variation in the trigeminal blink reflex and have shown that there are substantial individual differences in the sensitivity of this response to

323 changes in stimulus intensity. There is surprisingly little prior work that has measured how the
324 blink response varies with the intensity of a somatosensory stimulus. In a review of the clinical
325 assessment of the blink reflex, Esteban observed that increases in the current used to stimulate
326 the supraorbital nerve evoked larger and earlier EMG components from the orbicularis oculi
327 (which mirrors our findings) but this informal observation was not quantified (Esteban, 1999). In
328 perhaps the closest precedent for the current study, Flaten and Blumenthal found that varying
329 the intensity of an airpuff between 1.5 and 4.5 PSI resulted in a monotonic increase in the
330 amplitude of the EMG voltage response from the orbicularis oculi (Flaten & Blumenthal, 1998).
331 There have been studies of parametric variation in auditory (Peak, 1932) and visual stimulation
332 (Bixler *et al.*, 1967), which generally show an increase in amplitude and a decrease in blink
333 latency with increasing stimulus intensity. Overall, however, we are unaware of prior work that
334 has quantified how the form and timing of the blink changes with trigeminal stimulus intensity, or
335 how these changes covary within or across people.

336 *Comparison to EMG measures of the blink response*

337 EMG recording of the orbicularis oculi reveals temporally separated components of the blink
338 response. In primates, the early component (R1) is a small, ipsilateral reflex, while the later,
339 larger component (R2) is a bilateral response (Vollono, 2021). It is the R2 that that corresponds
340 with the actual blink of the eyelids (Rossi *et al.*, 1989) and is thus most related to our
341 measurements. A third, still later component (R3) has also been observed, particularly in
342 response to noxious stimuli (Rossi *et al.*, 1989). It is possible that the late squinting response
343 seen in some of our participants in response to the most intense (60 PSI) stimulus reflects the
344 R3 component.

345 *Interpretation of the trigeminal psychometric function*

346 We have shown that blink amplitude is well described by a two-parameter psychometric
347 function of the log of trigeminal stimulation intensity. It is likely that efferent neural activity within

348 the facial nucleus is linearly related to eyelid closure (Goodnight *et al.*, 1995). If so, stimulus
349 intensity undergoes a transformation from logarithmic to linear scale prior to this point. Such a
350 transformation has been observed, for example, between the transducing mechanoreceptors of
351 glabellar skin in the hand and the firing rate within the median and ulnar nerves (Muniak *et al.*,
352 2007), although down-stream targets of trigeminal afferents could also accomplish this
353 transformation (Buzsaki & Mizuseki, 2014).

354 The psychometric function is fully described by the threshold and slope parameters. An
355 intriguing but complicated topic concerns how properties of neural circuits give rise to the
356 particular values of these parameters that we measure in behavior. While such an analysis is
357 beyond the scope of the current study, we can find the outlines of a mechanistic account in
358 related areas of perceptual neuroscience. Studies of decision-making have examined how the
359 "readout" from populations of sensory neurons can give rise to psychometric response functions
360 of different forms (Gold & Ding, 2013). At the output stage the varying signals from a pool of
361 sensory neurons are selected, weighted, and combined; different mathematical operations that
362 perform this readout are predicted to produce different psychometric functions. Below, we draw
363 from this theoretical work to help interpret the variations in trigeminal sensitivity functions that
364 we have measured.

365 *Blink anatomy and ipsilateral and contralateral responses*

366 We find a systematic difference between the threshold parameters measured from the
367 eyelid ipsilateral and contralateral to the stimulus. That is, a higher intensity stimulus is required
368 to evoke a given amount of lid movement in the contralateral eye as compared to the ipsilateral
369 eye, consistent with prior work (VanderWerf *et al.*, 2003).

370 We might consider where and how this difference arises within the circuitry of the
371 trigeminal blink reflex. In the primate, corneal and eyelid sensory afferents arrive principally in
372 the spinal trigeminal nucleus pars caudalis and pars intermedius (May & Warren, 2021) These

trigeminal nuclei project to a circuit of neurons within the adjacent pontine reticular formation (PRF), which in turn project to output motor neurons in the ipsilateral and contralateral facial nucleus. The R2 blink response may arise from a reverberating signal within the PRF that ultimately drives the motor neurons (May & Warren, 2021). The amplitude of the R2 blink is strongly modulated by stimulus history (such as the habituation effects that we observe here) as well as numerous contextual manipulations such as pre-pulse inhibition (Powers *et al.*, 1997). The PRF is well positioned to be the site of this modulation, both from intrinsic circuit properties and from descending cortical inputs (Morcuende *et al.*, 2002).

A notable feature of our data is that, despite marked individual variation in overall threshold and slope, the threshold difference between the ipsilateral and contralateral blink response function is nearly identical across individuals (Figure 5b). This suggests that the increased contralateral threshold arises from a common neural mechanism across individuals, operating downstream from the source of individual variation.

Because of the logic of the measurement, the difference in sensitivity threshold between the ipsilateral and contralateral eyelid cannot arise within the trigeminal afferents or the output motor neurons. Instead, a plausible locus is within the neural circuitry of the PRF and its output to the motor neurons. For example, PRF projections might operate with reduced synaptic efficiency upon contralateral as compared to ipsilateral motor neurons, producing a fixed decrement in the spiking activity that drives the contralateral eyelid. We find that the contralateral blink is delayed by 4 milliseconds compared to the ipsilateral response (consistent with prior EMG measurements; (VanderWerf *et al.*, 2003). This latency could reflect a longer period of kindling of PRF circuit activity, additional synaptic stages, or both.

Individual differences in trigeminal blink sensitivity

We find that there are substantial individual differences in overall trigeminal sensitivity, as indexed both by half-response threshold and the slope of the response function. There is a

relatively strong correlation across individuals between these two parameters, suggesting that people vary in a primary sensitivity axis that impacts both of these parameters of the psychometric function. Given a set of neurons representing the stimulus, a non-linear readout rule that amplifies the influence of the weakest responding neurons upon motor output would be expected to flatten and shift the psychometric leftward, similar to the effect of a max pooling rule in decision making (Gold & Ding, 2013). We observe this kind of joint change in parameters across our participants, with the most sensitive individuals demonstrating a large blink response to even the smallest stimulus intensity, producing a low threshold and a shallow slope parameter.

The neural site of this variation could be present anywhere along the reflex pathway, although the spinal trigeminal nuclei and the PRF circuit are both plausible choices. Intrinsic network properties or extrinsic modulatory input to this system could produce the marked variation in overall sensitivity that we observe. For example, varying levels of tonic activity in the locus coeruleus neurons that project to and modulate the trigeminal nuclei could produce individual variation in the sensitivity of the blink response (Dauvergne *et al.*, 2008). This variation is present in a relatively homogeneous population of young adults without neurologic or ophthalmologic disease. An intriguing goal for future studies will be to identify behavioral or perceptual correlates of this variation and the neural source of the modulatory effect.

Applications and improvements

In other sensory domains, measurement of a stimulus-response function offers a fundamental characterization of sensitivity that can have clinical importance. For example, visual acuity measured over a range of stimulus contrast levels has been shown to better separate patients from controls in multiple sclerosis and predict changes in retinal and brain imaging measures (Balcer *et al.*, 2000). For the blink reflex, it is possible that measurement of an entire response function may more clearly reveal alterations in the sensitivity of the

trigeminal system in clinical disorders. An intriguing target is migraine, for which potentiation of pain signals from trigeminal afferents is a cardinal feature. Despite the apparent association between the trigeminal system and migraine, there is limited consensus regarding what (if any) alterations of somatic sensory processing accompany headache disorders (Coppola & Chen, 2021). EMG measures of the trigeminal blink response have been extensively studied in migraine, but with conflicting results regarding if an alteration in response is present (Vollono, 2021). It may be the case that these studies, performed at a single stimulus intensity level, have missed differences that would be revealed in the full trigeminal sensitivity function.

Our measurement of trigeminal sensitivity could be improved. First, the delivery of the airpuff is accompanied by an audible hiss. As the auditory stimulus alone can contribute to a blink response, future studies might have participants wear noise-cancelling headphones to remove this component. Second, while the precise timing of each airpuff trial could not be anticipated by the participant, it was the case that every trial presented a stimulus of one non-zero intensity or another. Participants may blink in anticipation of a stimulus, and this behavior might vary across individuals. The inclusion of acquisitions that do not present an airpuff would allow this behavior to be detected and modeled as part of the psychometric function.

Conclusions

Application of a psychometric framework to the trigeminal blink reflex has allowed us to efficiently summarize the effects of laterality, participant, and repetition upon a complex temporal response. This analysis framework yields parameters that may, in future work, be related to the properties of neural circuits in quantitative models. Finally, measurement and modelling in people with migraine and other clinical disorders may be used to test for disruptions of trigeminal sensitivity, and to attribute these alterations to particular neural mechanisms.

Author Contributions: Conceptualization: E.K., V.Y.B., and G.K.A. Data curation: G.K.A. Formal analysis: E.B.H. and G.K.A. Funding acquisition: V.Y.B. and G.K.A. Investigation: E.B.H. and D.P.G. Methodology: E.B.H. and G.K.A. Project administration: E.B.H. Resources: D.P.G. Supervision: D.P.G. and G.K.A. Visualization: E.B.H. and G.K.A. Writing - original draft: E.K., E.B.H., and G.K.A. Writing - review & editing: E.K., E.B.H., D.P.G., V.Y.B., and G.K.A.

Acknowledgements: none

Study Funding: P30 EY001583: Core Grant for Vision Research. In kind support provided by BlinkTBI Inc., including hardware, initial video processing, and engineering expertise.

Declaration of conflicting interest: none

References

Aguirre GK, Mattar MG & Magis-Weinberg L. (2011). de Bruijn cycles for neural decoding. *Neuroimage* **56,** 1293-1300.

Balcer LJ, Baier ML, Pelak VS, Fox RJ, Shuwairi S, Galetta SL, Cutter GR & Maguire MG. (2000). New low-contrast vision charts: reliability and test characteristics in patients with multiple sclerosis. *Mult Scler* **6,** 163-171.

Bixler EO, Bartlett NR & Lansing RW. (1967). Latency of the blink reflex and stimulus intensity. *Percept Psychophys* **2,** 559-560.

Buzsaki G & Mizuseki K. (2014). The log-dynamic brain: how skewed distributions affect network operations. *Nat Rev Neurosci* **15,** 264-278.

Coppola G & Chen W-T. (2021). *Neurophysiology of the Migraine Brain*. Springer, Cham :.

Dauvergne C, Smit AE, Valla J, Diagne M, Buisseret-Delmas C, Buisseret P, Pinganaud G & Vanderwerf F. (2008). Are locus coeruleus neurons involved in blinking? *Neurosci Res* **61,** 182-191.

Esteban A. (1999). A neurophysiological approach to brainstem reflexes. Blink reflex. *Neurophysiol Clin* **29,** 7-38.

Flaten MA & Blumenthal TD. (1998). A parametric study of the separate contributions of the tactile and acoustic components of airpuffs to the blink reflex. *Biol Psychol* **48,** 227-234.

Gold JI & Ding L. (2013). How mechanisms of perceptual decision-making affect the psychometric function. *Prog Neurobiol* **103,** 98-114.

Goodnight JW, Dulguerov P, Berke GS, Lesavoy M & Hoffman LF. (1995). Correlation of compound action potential and electromyography with facial muscle tension. *Otolaryngol Head Neck Surg* **112,** 279-290.

May PJ & Porter JD. (1998). The distribution of primary afferent terminals from the eyelids of macaque monkeys. *Exp Brain Res* **123,** 368-381.

May PJ & Warren S. (2021). Macaque monkey trigeminal blink reflex circuits targeting orbicularis oculi motoneurons. *J Comp Neurol* **529,** 2842-2864.

Morcuende S, Delgado-Garcia JM & Ugolini G. (2002). Neuronal premotor networks involved in eyelid responses: retrograde transneuronal tracing with rabies virus from the orbicularis oculi muscle in the rat. *J Neurosci* **22,** 8808-8818.

Muniak MA, Ray S, Hsiao SS, Dammann JF & Bensmaia SJ. (2007). The neural coding of stimulus intensity: linking the population response of mechanoreceptive afferents with psychophysical behavior. *J Neurosci* **27,** 11687-11699.

Peak H. (1932). Intensity of stimulation and the amplitude and latency of the lid-reflex. *The American Journal of Psychology* **44,** 785-788.

Powers AS, Schicatano EJ, Basso MA & Evinger C. (1997). To blink or not to blink: inhibition and facilitation of reflex blinks. *Exp Brain Res* **113,** 283-290.

Rossi B, Risaliti R & Rossi A. (1989). The R3 component of the blink reflex in man: a reflex response induced by activation of high threshold cutaneous afferents. *Electroencephalogr Clin Neurophysiol* **73,** 334-340.

VanderWerf F, Brassinga P, Reits D, Aramideh M & Ongerboer de Visser B. (2003). Eyelid movements: behavioral studies of blinking in humans under different stimulus conditions. *J Neurophysiol* **89,** 2784-2796.

Vollono C. (2021). Brainstem Reflexes. In *Neurophysiology of the Migraine Brain*, ed. Coppola G & Chen W-T. Springer, Cham :.

Wichmann FA & Hill NJ. (2001). The psychometric function: I. Fitting, sampling, and goodness of fit. *Percept Psychophys* **63,** 1293-1313.

Title: Parametric modulation of blink response as an individual difference measure of trigeminal sensitivity

Running head: Psychometric Blink

Author(s):
Eric Kaiser[†]; Edda B Haggery[†], Dena P Garner, Vatinee Y Bunya, Geoffrey K Aguirre*

[†]These authors contributed equally

[*]**Corresponding Author:**
Geoffrey K Aguirre
3400 Spruce Street, Philadelphia, PA 19104
aguirreg@upenn.edu

SUPPLEMENTARY MATERIALS

The design of our study was the subject of a pre-registered protocol (https://github.com/gkaguirrelab/preregistrations/tree/master/blink_2021). Here, we present the results of the pre-registered analysis approach.

Methods

At the first stage of analysis, trials that contained a "valid" blink were identified, using a lid movement criterion defined within the BlinkCNS proprietary analysis software. The valid trials were retained, and a measure of nine blink "features" was derived from the recording made from the eye ipsilateral to the air puff stimulus. These features were:

- Area-under-the-curve (AUC) (msecs * pixels): Mean area-under-the-curve of the trajectory of the eyelid between the onset and completion of the blink as measured relative to the tonic position for that blink.
- Latency (msecs): Mean elapsed time between the application of the stimulus and the detection of the blink onset.
- Time under 20 (msecs): Mean elapsed time between the eyelid reaching a closed position and the eyelid moving more than 20 pixels back towards the tonic position.

- Time to open (msecs): Mean elapsed time between the eyelid reaching a closed position and the eyelid returning within threshold of the tonic position.
- Initial velocity (pixels / msecs): Mean average velocity over the first 7 frames of the blink.
- Time to close (msecs): Mean elapsed time between the detection of the onset of the blink and the eyelid reaching a closed position.
- Max closing velocity (pixels / msecs): Mean maximum velocity of the eyelid between the detected onset of the blink and the eyelid reaching the closed position.
- Max opening velocity (pixels / msecs): Mean maximum velocity of the eyelid between the eyelid reaching the closed position and the eyelid returning within threshold of the tonic position.
- Blink rate (count): Number of blinks performed by the eyelid between stimuli.

An acquisition was retained if it contained at least three valid blinks; the mean value for each feature from all valid trials within an acquisition was obtained. For each blink feature, we fit a linear model that related the log of the realized air pressure to the values of the blink feature, using the data from all acquisitions for the subject. A robust linear regression (the *fitlm* MATLAB function) was used to calculate the fit. The parameters of the fit were expressed as the slope of the relationship between log pressure and the blink feature, and as an offset value, which was the fitted value for the blink feature at 15 PSI.

The fit was performed first using the entire potential set of 50 acquisitions combined across the two testing sessions; for each subject we retained the R^2 of the model fit to the data for each feature. The sign of the slope of the model fit for each subject and blink feature was assigned to the R^2 value, supporting an examination of the mean, across subject, signed R^2 value as a test of the ability of the model to reliably account for experimental variance.

The reproducibility of these parameter values was examined by performing the linear model fit separately for the data from each of the two sessions, standardizing and grouping the resulting parameters across blink features, and then calculating the Pearson's r value between the session 1 data and session 2 data across participants.

Results

	Puff pressure model (R^2)	**Test-retest slope (r)**	**Test-retest slope (IQR)**	**Test-retest offset (r)**	**Test-retest offset (IQR)**
AUC	**0.81** [0.68, 0.92]	**0.78** [0.28, 0.99]	**33** [6, 116]	**0.64** [0.49, 0.99]	**16** [3, 278]
Latency	**0.98** [0.97, 0.98]	0.81 [-0.13, 0.98]	**24** [8, 51]	**0.92** [0.77, 0.99]	4 [0, 11]
Time under 20	**0.84** [0.76, 0.89]	-0.08 [-0.48, 0.96]	**57** [16, 1973]	0.17 [-0.14, 0.98]	**55** [12, 455]
Time to open	**0.79** [0.66, 0.90]	**0.82** [0.25, 0.99]	**59** [15, 133]	**0.61** [0.46, 0.99]	**38** [2, 231]
Initial velocity	**0.68** [0.53, 0.82]	**0.70** [0.09, 0.98]	**55** [10, 201]	**0.91** [0.77, 0.98]	**10** [4, 15]
Time to close	**0.43** [0.25, 0.61]	**0.79** [0.45, 0.99]	**131** [30, 249]	**0.73** [0.12, 0.97]	**8** [3, 16]
Close velocity	**0.72** [0.56, 0.85]	**0.89** [0.62, 1.0]	**31** [5, 137]	**0.90** [0.66, 0.98]	**11** [4, 20]
Open velocity	**0.58** [0.49, 0.69]	**0.86** [0.39, 0.99]	**35** [11, 107]	**0.75** [0.13, 0.96]	**14** [5, 37]
Blink rate	**0.58** [0.41. 0.74]	**0.56** [0.16, 9.91]	**132** [31, 633]	**0.85** [0.73, 0.96]	**34** [7, 51]

Table 1. Overview
Correlations and test-retest reliability by blink feature as a function of puff pressure. 95% CIs are described in brackets. Values for which the 95% CI excludes zero are bolded. *Column 1*: Pearson's R^2 for the blink feature as a function of log puff pressure combined across sessions. The value shown is the mean R^2 across subjects. *Column 2*: Mean test-retest reliability in the slope of the fit linear regression model for subjects between sessions 1 and 2. *Column 3:* Interquartile range for the slope agreement between sessions 1 and 2. *Column 4:* Mean test-retest reliability in the offset of the fit linear regression model for subjects between sessions 1 and 2. *Column 5:* Interquartile range for the offset agreement between sessions 1 and 2.